4110 *Macromolecules* **2009**, *42*, 4110–4117
DOI: 10.1021/ma9001929

Macromolecules
ARTICLE

Stable Hydrogen-Bonding Complexes of Poly(4-vinylpyridine) and Polydiacetylenes for Photolithography and Sensing

Si Wu,[†,‡] Feng Shi,[†,§] Qijin Zhang,*[,‡] and Christoph Bubeck*[,†]

[†]*Max Planck Institute for Polymer Research, Ackermannweg 10, 55128 Mainz, Germany, and* [‡]*CAS Key Laboratory of Soft Matter Chemistry, Department of Polymer Science and Engineering, University of Science and Technology of China, Key Laboratory of Optoelectronic Science and Technology in Anhui Province, Hefei, Anhui 230026 P. R. China.* [§] *Present address: Key Lab for Nanomaterials, Beijing University of Chemical Technology, Beijing 100029, P. R. China.*

Received January 29, 2009; Revised Manuscript Received April 10, 2009

ABSTRACT: We prepare hydrogen-bonding complexes of the diacetylene derivatives 10,12-tricosadiynoic acid, 4,6-heptadecadiynoic acid, and ((*E*)-4-((4-(tricosa-10,12- diynoyloxy)phenyl)diazenyl)benzoic acid and poly(4-vinylpyridine) in organic solvents. The complexes are spin-cast and form high-quality thin films, which can be photopolymerized and yield the blue phase of polydiacetylenes. A cross-linked network of the hydrogen-bonding complex is formed and shows improved stability to organic solvents. We demonstrate sensor capabilities for various organic solvents and gases by means of the blue-to-red color changes of polydiacetylenes. Based on the different solubility of the hydrogen-bonding complex before and after UV irradiation, photolithography can be employed to fabricate microstructures for polydiacetylene-based devices.

1. Introduction

Hydrogen bonding is one of the most useful interactions in the fabrication of functional supramolecular complexes due to its directionality and moderate strength.[1−3] A large variety of functional materials can be fabricated by hydrogen bonding.[4] Furthermore, the stabilities of biomaterials, optoelectronic materials, and many other materials can be improved by hydrogen bonding.[5]

Polydiacetylenes (PDAs) are well-known conjugated polymers, which show intense colors due to their highly delocalized, one-dimensional π-electron system of their polymer backbone. Most PDAs appear with an intense blue color related to an absorption maximum at the wavelength λ_{max} around 640 nm. Many stimuli cause a color change to a red phase with λ_{max} around 550 nm, such as temperature,[6−9] pH,[10] stress,[11] ions,[12] solvents,[7,13] and ligand interactions.[14] The intriguing stimuli-responsive color changes of PDAs have potential applications as sensors, molecular switches,[6−8,12,14,15] and many others in optoelectronics.[16]

The applications described above usually require thin films of PDAs which must be stable to several solvents; i.e., the films must adhere well to the substrate and must not undergo any changes of the morphology upon exposure to the solvents. But this is a frequent problem.[17,18] Two attempts were made to fabricate PDA films with improved solvent stability. The first is using molecules containing two diacetylene moieties to fabricate cross-linked Langmuir−Blodgett films of PDAs.[17,19] However, the Langmuir−Blodgett technique has many problematic limitations.[20] Spin-coating of diacetylene monomers, on the other hand, is not appropriate and does not provide satisfactory results because their molecular weight is usually small. The second method is to introduce diacetylene monomers into the network of silica by the sol−gel method.[7,18,21] Although this provides good films, the gel is already insoluble before the diacetylenes are polymerized. Therefore, it is not possible to fabricate microstructures by photolithography because this would need to dissolve the unpolymerized part of the film by solvents. Therefore, it is highly desirable to find an alternate method to fabricate solvent stable PDA films by spin-coating, which are suitable for photolithography.

The aim of our work is to demonstrate a new strategy to fabricate thin films of diacetylenes by spin-coating. They are photopolymerized subsequently, become insoluble in common solvents, and can be used to fabricate microstructures by photolithography. Our stabilization concept is based on hydrogen bonding between diacetylene monomers which contain a carboxylic group (DA, hydrogen donor) and poly(4-vinylpyridine) (P4VP, hydrogen-bonding acceptor). We prepare thin films by spin-coating of the hydrogen-bonding complex P4VP−DA. Because of the large molecular weight of P4VP, the film-forming property of the complex is very good. Homogeneous and highly transparent films can be obtained this way. Thin films of this hydrogen-bonding complex show different solubility of the unpolymerized and polymerized parts. Consequently, photolithography can be used to fabricate patterns, which enable PDA-based devices with improved stability. The stable hydrogen-bonding complex will also be used as sensor for organic solvents and gases.

2. Experimental Section

2.1. Materials. 10,12-Tricosadiynoic acid (TDA), 4,6-heptadecadiynoic acid (HDA), poly(4-vinylpyridine) (P4VP, M_w = 60 000), and poly(styrene) (PS, M_w = 71 000) are all commercially available. ((*E*)-4-((4-(Tricosa-10,12-diynoyloxy)phenyl)diazenyl)benzoic acid (AzoDA) is synthesized according to our previous work.[22] The chemical structures of the materials are shown in Scheme 1. It is well-known that hydrogen bonds will form between the acids (hydrogen-bonding

*Corresponding authors. E-mail: zqjm@ustc.edu.cn (Q.Z.); bubeck@mpip-mainz.mpg.de (C.B.).

 Published on Web 04/29/2009

Scheme 1. Chemical Structures and Names of the Used Materials

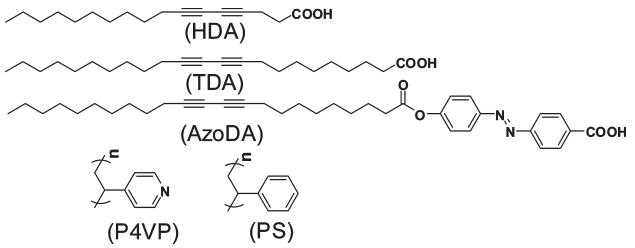

donors) and the nitrogen atoms of P4VP, which act as hydrogen-bonding acceptors. PS is used for control experiments because it cannot form hydrogen bonds with the acids HDA, TDA, and AzoDA.

2.2. Preparation of the Thin Films. The diacetylene-containing acids (HDA or TDA) and P4VP are dissolved in ethanol using always the same molar ratio 1:1 between the carboxyl and the pyridine groups. DMF is used analogously to dissolve AzoDA and P4VP. The solutions are sonicated for 5 min and then stirred for several hours before use. Thin films of the hydrogen-bonding complex are prepared by spin-coating this solution on freshly cleaned glass substrates. The film thickness d can be controlled by appropriate choice of spinning speed ω and concentration C of the solution using the empirical equation for the thickness of two films[23]

$$d_2 = d_1(\omega_2/\omega_1)^{\alpha}(C_2/C_1)^{\beta} \quad (1)$$

with exponents α and β to be determined experimentally for the individual materials. After spin-coating, the films are dried in an oven under vacuum at room temperature for about 4 h. Subsequently, the film thickness is measured with a step-profiler (Tencor Instruments model P-10). Here, we present the details of film fabrication of P4VP−TDA as an example. We prepare two solutions. Solution 1: 9 mg of P4VP and 30 mg of TDA are dissolved in 2 mL of ethanol. Solution 2: 15 mg of P4VP and 50 mg of TDA are dissolved in 2 mL of ethanol. These solutions are spin-cast at different spinning speeds. For solution 1, ω = 1000 and 3000 rpm result in films with average thickness of 156.8 and 100.2 nm, respectively. For solution 2 and ω = 3000 rpm, we get a film thickness of 203.2 nm. This yields exponents α = −0.41 and β = 1.38. By rearranging eq 1, we determine the appropriate spinning speeds for films with defined thicknesses for photolithography (typical d = 50 nm) and for small-angle X-ray diffraction measurements (typical d = 180 nm).

The polymerization of P4VP−TDA is carried out at room temperature by irradiating the films with an ordinary UV hand lamp at 254 nm.

2.3. Measurements. ^{1}H NMR spectra are measured on a Bruker 250 MHz NMR spectrometer at room temperature. In the ^{1}H NMR spectra measurements, P4VP, TDA, and hydrogen-bonding complex P4VP−TDA with molar ratio 1:1 are all dissolved in DMSO-d_6. The solutions of TDA in DMSO-d_6 and P4VP−TDA in DMSO-d_6 are prepared with the same concentration of TDA of 20 mg/mL. UV−vis absorption spectra are measured on a Perkin-Elmer Lambda 900 UV−vis spectrometer. Images of the optical microscopy, polarized optical microscopy, and fluorescent microscopy are all recorded on a Zeiss Axiophot microscope. Small-angle X-ray diffraction (SAXD) patterns are measured on a Phillips goniometer PW 1820 system with Cu Kα line (λ = 0.154 18 nm). Raman spectra are measured with a LABRAM-HR confocal micro-Raman spectrometer using a semiconductor laser at 785 nm. Infrared spectra are obtained using a Nicolet 730 FT-IR spectrometer using ATR mode.

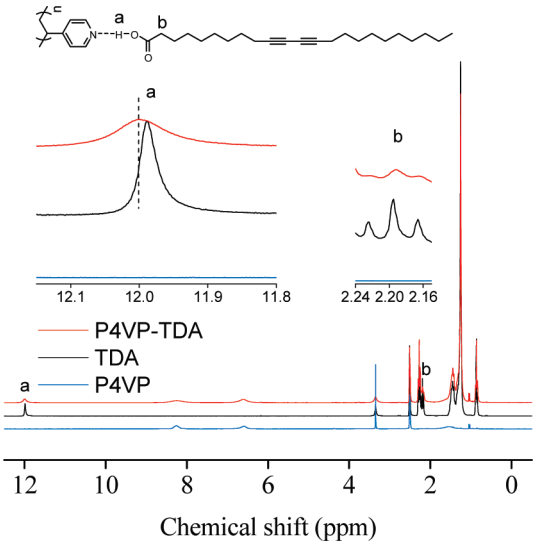

Figure 1. ^{1}H NMR spectra of P4VP, TDA, and the hydrogen-bonding complex of P4VP−TDA. Insets show the chemical structure, enlargement of signals of the proton on carboxylic group of TDA (proton "a"), and the proton nearest to the carboxylic group of TDA (proton "b").

3. Results and Discussion

3.1. Structure and Stability of the Hydrogen-Bonding Complex. It is well-known that carboxylic groups and pyridine groups have a tendency to self-assemble and form hydrogen bonds.[24−26] The formation of hydrogen bonds between carboxylic groups and pyridine groups in P4VP−TDA is proved by ^{1}H NMR spectra. The ^{1}H NMR spectra of TDA, P4VP, and P4VP−TDA are shown in Figure 1. Proton "a" is the proton on the carboxylic group of TDA. The signal of proton "a" is at around 12 ppm. Without P4VP, the signal of proton "a" is a sharp peak. After P4VP and TDA are mixed in the molar ratio 1:1, the peak of proton "a" shifts downfield, and the peak broadens significantly. The shift and broadening indicate formation of hydrogen bonding.[27] Proton "b" is the proton which is nearest to the place where hydrogen bonding forms. The signal of proton "b" in P4VP−TDA undergoes obvious broadening compared with that of pure TDA, which is also an indication of formation of hydrogen bonding.[28] Lu et al. also reported similar broadening effect in ^{1}H NMR spectra when they studied the self-assembly property of a small guest molecule with a polymer host.[29]

The FT-IR spectra of thin films of P4VP−TDA, TDA, and P4VP were measured using ATR mode. The IR spectra of TDA and P4VP−TDA show a strong band at 1691 cm^{-1} which corresponds to the carboxylic acid (see Supporting Information). We do not see any indication of carboxylate bands in the IR spectrum as observed in earlier work.[30] Therefore, we can rule out the possibility of a complex between a carboxylate ion with the proton going to the pyridine, as would be expected in case of a polyion−surfactant complex.

On the basis of the results of NMR and IR spectroscopy, we conclude that the P4VP−TDA complex is caused by hydrogen bonding. Scheme 2 shows a model of the P4VP−TDA hydrogen-bonding complex. We assume that TDA self-assembles and forms microcrystalline domains in the hydrogen-bonding complex.

The polymerization of TDA in films of the hydrogen-bonding complex is performed by UV irradiation at 254 nm, which causes the characteristic absorption peak of the blue phase PDA at around 640 nm as shown in Figure 2. The

Scheme 2. Schematic Model of the Hydrogen-Bonding Complex P4VP−TDA and the Network Formation after Photopolymerization in the Hydrogen-Bonding Complex P4VP−PolyTDA

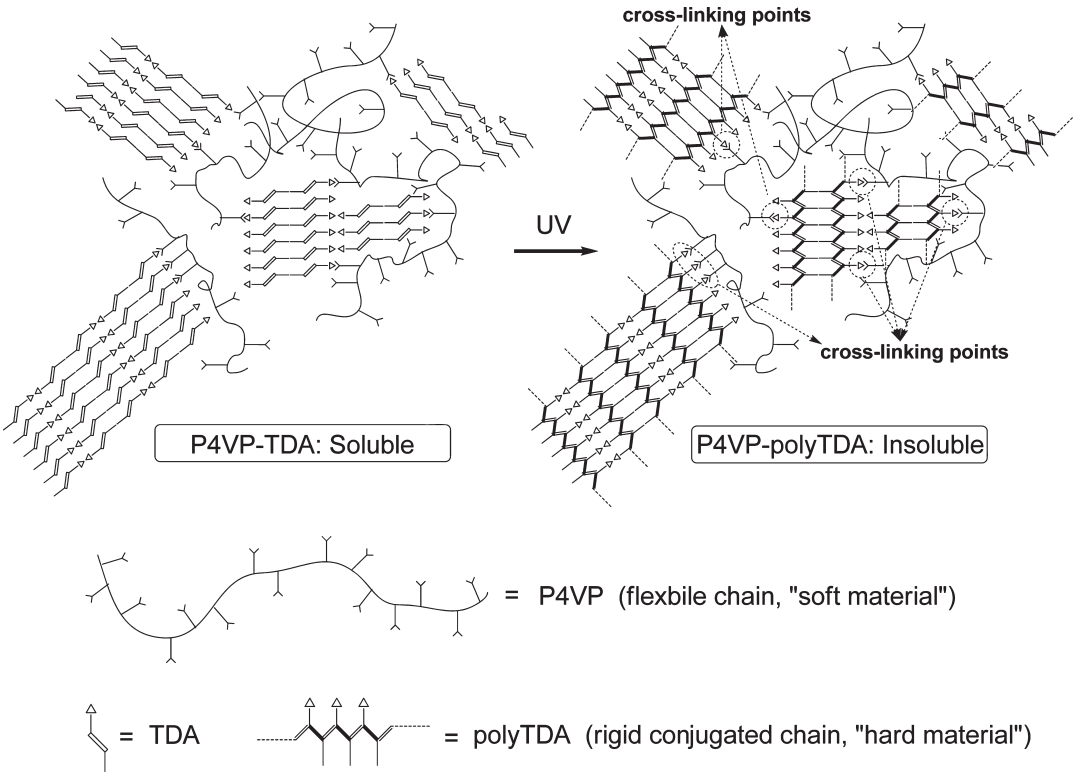

mechanism of photopolymerization of diacetylene is a topochemical reaction.[31,32] The polymerization happens in close-packed structures, such as crystals,[31,32] monolayers,[33] Langmuir−Blodgett films,[30,34] liposomes,[35] micelles, or vesicles.[35] Obviously, the microenvironment of the hydrogen-bonding complex is suitable for the topochemical reaction, which is proved by the characteristic absorption band of PDA. Further evidence for the polymerization is obtained by Raman spectroscopy of thin films of P4VP−TDA, which shows the characteristic bands at 1451 and 2084 cm^{-1} after UV irradiation, corresponding to the C=C and C≡C stretching vibrations of the PDA backbone, respectively. As the samples become insoluble after the UV irradiation, standard methods of molecular weight determination such as GPC are not appropriate to analyze the molecular weight and degree of polymerization. As we see a well-resolved vibronic structure in the absorption spectra and do not recognize any indication for oligomers at shorter wavelengths as reported in earlier work,[32] we can conclude only that we observe PDA chains longer than typical oligomers.

The textures of thin films with a typical thickness of about 180 nm are studied by polarized optical microscopy (POM) and shown in Figure 3. The POM image of P4VP is dark, which indicates that P4VP does not form crystalline structures. Films of polyTDA alone show spherulite-like crystals whose sizes are from < 100 μm to several hundred micrometers. The hydrogen-bonding complex P4VP−polyTDA forms very tiny crystals which have typical sizes of several micrometers or less. The texture of P4VP−polyTDA is different than the textures of both constituents alone. This observation is in line with earlier reports that the film morphologies of hydrogen-bonding complexes are quite different to those of the hydrogen-bonding acceptors or donors alone.[26,36]

To have a better understanding of the crystalline structures shown in Figure 3, the small-angle X-ray diffraction (SAXD) patterns are measured with the same films already used for POM measurements. Figure 4 shows the SAXD patterns of P4VP, polyTDA, and P4VP−polyTDA. There is no diffraction peak in the P4VP film. The SAXD result and the dark POM image of P4VP indicate that P4VP is amorphous in the film. It is known that PDAs can easily form bilayer structures.[30,31,35,37,38] There are several strong Bragg peaks in the diffraction pattern of polyTDA. We observe a lamellar thickness of polyTDA film of 4.18 ± 0.02 nm, which is calculated by Bragg's law taking the average of the diffraction peaks displayed in Figure 4.

The length of the fully extended side chain of polyTDA is about 2.7 nm, which is calculated by the optimized MM2 model using ChemBioOffice 2008. Obviously, the lamellar thickness of polyTDA is smaller than the bilayer thickness of polyTDA calculated for the case of perpendicular alkyl chains which are fully extended. So, the side chains of polyTDA must be in a bent conformation or, more likely, in their extended conformation with the side chain axes titled with respect to the layer planes.[38] There are also several Bragg peaks in the diffraction pattern of the P4VP−polyTDA film. Compared with the diffraction pattern of polyTDA, there are two major differences.

The first difference is that the Bragg peaks in P4VP−polyTDA are shifted to lower angles. We derive a lamellar thickness of P4VP−polyTDA of 4.28 ± 0.03 nm, which is bigger than that of polyTDA. There could be several reasons for the enlargement of the lamellar thickness. P4VP may get partly inserted between the layers of polyTDA when they form hydrogen bonds. Another possible reason is that hydrogen bonding is a force which pulls the side chain of polyTDA to a more extended conformation. The third possible reason is that hydrogen bonding changes the tilt angle of the side chains of polyTDA with respect to the layer planes. Although the detailed mechanism of the lamellar

thickness increase is not clarified yet, the appearance of the hydrogen bonding plays an important role.

The second difference in the diffraction patterns is that the intensity of the diffraction of P4VP−polyTDA is less than 1/10 of the intensity of polyTDA. The thickness of both polyTDA and P4VP−polyTDA films is about 180 nm, and the concentration of polyTDA in P4VP−polyTDA is about 77 wt %. So, we do not think the film thickness and the concentration of polyTDA are the main reasons for the different diffraction intensity. As shown in Figure 3, polyTDA forms much larger crystalline domains compared with P4VP−polyTDA. The result indicates the degree of crystallization in polyTDA is higher. The much weaker diffraction intensity in P4VP−polyTDA is probably caused by the lower degree of crystallization.

Scheme 2 shows a schematic model of the hydrogen-bonding complex. The hydrogen-bonding complex forms a cross-linked network after photopolymerization. Therefore, P4VP−polyTDA is expected to have improved stability. Figure 5a shows photos of the blue films of P4VP−polyTDA (left) and polyTDA (right). After exposure to ethanol, both films turn red, which is the well-known solvent-induced color change of PDAs.[7,13,18] Figure 5b shows photos of P4VP−polyTDA film (left) and polyTDA film (right) after exposure to ethanol for 1 min. P4VP−polyTDA film shows stability to ethanol, but ethanol partly destroys the polyTDA film if it is not stabilized by P4VP. Other research groups also reported that PDA films without any stabilization mechanism were destroyed by solvents,[17,18] which is similar to our observations. After exposure to ethanol for 40 min, the P4VP−polyTDA film is still stable whereas the polyTDA film is totally destroyed by ethanol (see Figure 5c). These photos clearly demonstrate that hydrogen bonding improves the stability of polyTDA to the organic solvent considerably.

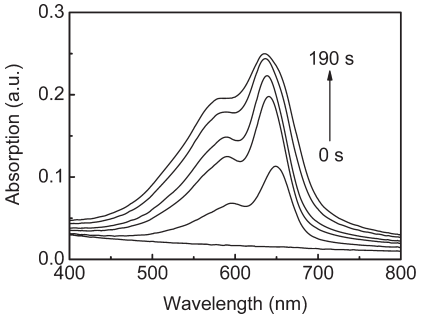

Figure 2. UV−vis absorption spectra of a P4VP−TDA film recorded after various irradiation times of UV light at 254 nm.

As a control experiment, we used PS instead of P4VP because PS cannot form a hydrogen-bonding complex with TDA. The common solvent of PS and TDA is cyclopentanone. The details of our results are shown in the Supporting Information. After exposure to cyclopentanone for only 1 min, the PS−polyTDA film is partly destroyed. The absorption of PS in the film PS−polyTDA is also reduced remarkably after washing by cyclopentanone for several minutes. The control experiment confirms that polyTDA is not stable to the solvent without hydrogen bonding.

We conclude that the improved stability of P4VP−polyTDA is caused by two contributions.

1. The hydrogen bonds act as cross-linking points between P4VP and polyTDA, as shown in Scheme 2. The chain segments of polyTDA are attached to P4VP by hydrogen bonding and form a cross-linked network in P4VP−polyTDA which improves the stability of the complex. Therefore,

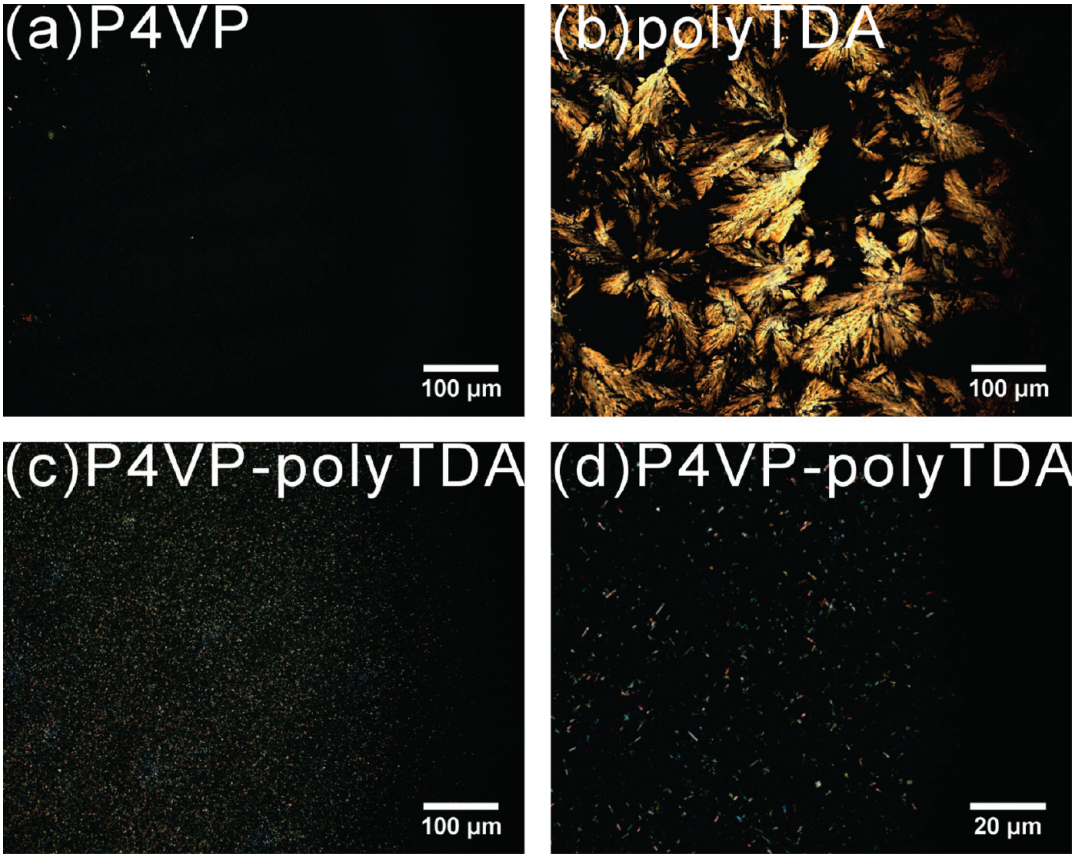

Figure 3. Polarized optical microscopy (POM) images of spin-coating films of (a) P4VP, (b) polyTDA, (c) P4VP−polyTDA, and (d) enlargement of the image of P4VP−polyTDA.

it is not possible anymore to dissolve P4VP−polyTDA in ethanol.

2. Apparently, polyTDA has a higher degree of crystallization compared to P4VP−polyTDA, as suggested by its larger crystalline domains and much stronger X-ray diffraction intensity. It was argued that this might result in the formation of sharp domain boundaries and packing defects, leading to a low stability of the film on the substrate.[17] In P4VP−polyTDA, the case is different as polyTDA has a rigid conjugated polymer chain and P4VP has much more flexible polymer chain. Natural materials such as bone and shell and other man-made materials that combine hard and soft materials can result in composite materials with enhanced mechanical and thermal properties.[7,39] According to the two kinds of chain structures of P4VP and polyTDA and the morphology shown in Figure 3c,d, the P4VP−polyTDA system appears just like combining hard and soft materials. This way, an improved stability of this system can result.

3.2. Sensing Properties of the Hydrogen-Bonding Complex. The stability to the solvent and solvent-induced color change property of the hydrogen-bonding complex provide the possibility that the complex can be used as a sensor for solvents. We use the other two hydrogen-bonding complexes P4VP−polyHDA and P4VP−polyAzoDA for comparison. Films of P4VP−polyTDA, P4VP−polyHDA, and P4VP−polyAzoDA are exposed to different solvents. Some films show color changes which are related to the well-known blue-to-red color changes of PDAs.[7,13,18] The photo is shown in Figure 6a, and the corresponding UV−vis absorption spectra are displayed in Figure 6b−d. The P4VP−polyHDA films turn red after exposure to the solvents, which show typical red phase PDA absorption bands at 400−600 nm. The P4VP−polyTDA films turn red after exposure to ethyl acetate, ethanol, and THF. The P4VP−polyTDA film turns purple but not red after exposure to hexane, which shows both red and blue phases of the PDA absorption bands. The P4VP−polyAzoDA films keep blue after exposure to the organic solvents shown in Figure 6 and many other solvents, such as DMF and acetone. As we know, the aggregation of the azo chromophores improves the stability of the conjugated backbone of polyAzoDA.[22] The property of P4VP−polyAzoDA films presented here is unique and different from the other PDAs.[7,13,18] The unique stability of P4VP−polyAzoDA may lead to applications in optoelectronic devices.

When used in combination, these systems allow for visual differentiation of organic solvents by simply monitoring the color changes. The organic solvent-induced color changes in the hydrogen-bonding complexes are irreversible and stay nearly unchanged for at least a week. The vivid color changes to organic solvents, which can be observed by the naked eye, are one of the major advantages of PDA-based sensor systems. The number of distinguishable organic solvents should increase when a combination of structurally diverse diacetylene derivatives are used. As a kind of self-assembled donor−acceptor system, our system is easily tunable by varying the diacetylene derivatives.

The hydrogen-bonding complex P4VP−polyTDA also has other stimuli-responsive properties. For example, P4VP−polyTDA shows a color change after exposure to special gases. Figure 7 presents the UV−vis spectra of P4VP−polyTDA films after exposure to different gases for 15 min. The color of the film exposed by ammonia changes to red, which is related the absorption band of the typical red phase PDA. The films exposed to the other gases keep blue. This result indicates that P4VP−diacetylene complexes also have gas sensing properties.

3.3. Fabrication of Microstructures of the Hydrogen-Bonding Complex. Different solubilities of materials before and after polymerization are a general prerequisite for photolithography. Therefore, we perform the following experiments to demonstrate the different solubilities of P4VP−TDA and P4VP−polyTDA. Thin films of the hydrogen-bonding complex before and after polymerization are exposed to ethanol, the common solvent of P4VP and TDA. The UV−vis absorption spectra of the thin films before and after exposure to ethanol for certain times are shown in Figure 8. Figure 8a shows the absorption spectra of the complex before polymerization. The absorption band of pyridine groups in P4VP is seen in the UV range. After exposure to ethanol, the absorption band in Figure 8a gradually decreases, which indicates that the unpolymerized complex is dissolved in ethanol. On the other hand, the polymerized complex cannot be dissolved anymore in ethanol as is shown in Figure 8b. After exposure to ethanol, the color of P4VP−polyTDA immediately changes to red. This is the well-known solvent-induced color change of PDAs.[7,13,18] The absorption band in the UV range does not show any decrease after exposure in ethanol for 10 min, which indicates that P4VP in P4VP−polyTDA cannot be dissolved in ethanol. As we know, pure P4VP

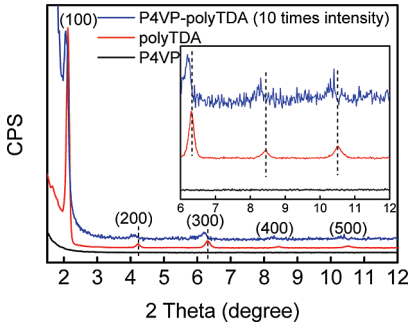

Figure 4. Small-angle X-ray diffraction (SAXD) patterns of thin films of P4VP, polyTDA, and P4VP−polyTDA. The inset is an enlargement of the SAXD patterns of 2θ between 6° and 12°. The intensity of P4VP−polyTDA is multiplied for 10 times.

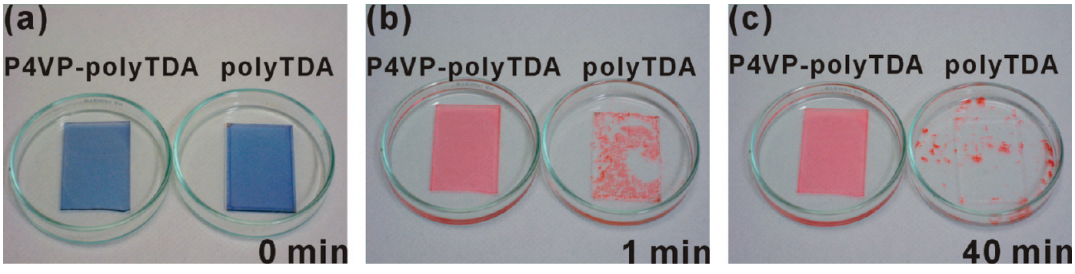

Figure 5. Photographs of (a) films of P4VP−polyTDA (left) and polyTDA (right), (b) films of P4VP−polyTDA (left) and polyTDA (right) after exposure in ethanol for 1 min, and (c) films of P4VP−polyTDA (left) and polyTDA (right) after exposure in ethanol for 40 min.

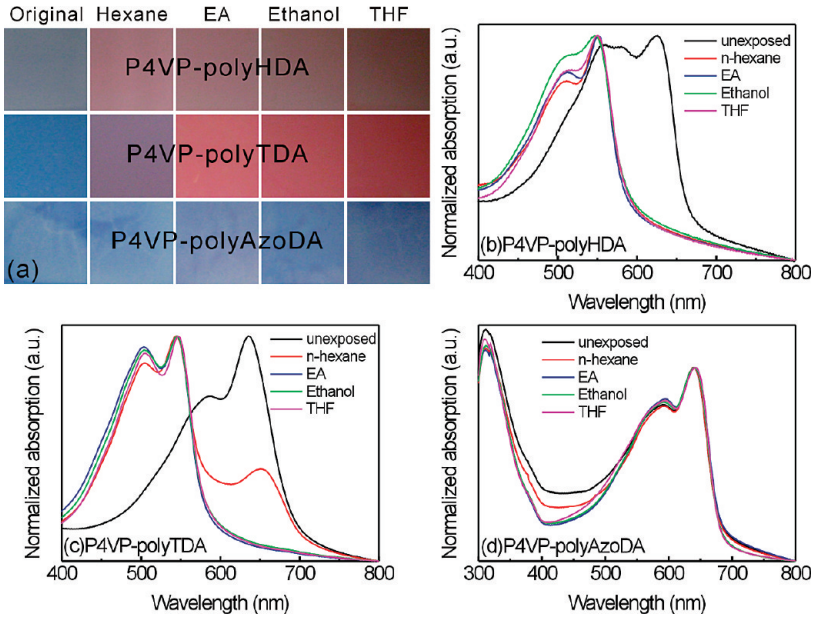

Figure 6. (a) Photographs of hydrogen-bonding complexes of P4VP−polyHDA, P4VP−polyTDA, and P4VP−polyAzoDA before and after exposure to different organic solvents. The films at left are unexposed ones and the ones to the right side are after exposure to *n*-hexane, ethyl acetate (EA), ethanol, and THF. UV−vis absorption spectra of (b) P4VP−polyHDA films, (c) P4VP−polyTDA films, and (d) P4VP−polyAzoDA films before and after exposure to different organic solvents.

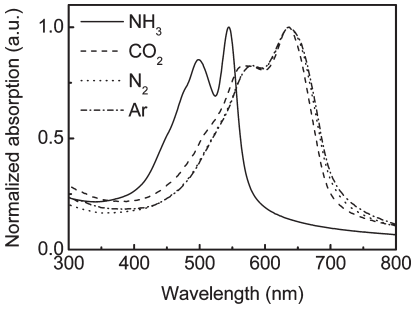

Figure 7. UV−vis absorption spectra of P4VP−polyTDA films after exposure to different gases for 15 min.

has good solubility in ethanol. The insolubility of P4VP in the hydrogen-bonding complex P4VP−polyTDA shows again that the cross-linked hydrogen-bonding complex improves the stability of P4VP to the solvent. The absorption band at 400−600 nm is attributed to the red phase of PDA. The absorption band of the red phase of PDA also does not change after various exposure times in ethanol from 1 to 10 min. This again shows that P4VP−polyTDA is quite stable to ethanol.

The different solubility of the hydrogen-bonding complex before and after polymerization ensures that PDA-based microstructures and devices can be fabricated by photolithography. Here, we generate a typical microscopic pattern of P4VP−polyTDA by photolithography as an example. The fabrication of the pattern is explained in Figure 9. In the first step, P4VP−TDA film is irradiated by UV light at 254 nm and the exposed area is polymerized. As shown in Figure 9a, this process results in a pattern of blue areas. Since PDA in the blue phase is nonfluorescent,[6] no patterned fluorescent images can be observed (see Figure 9b). In the second step, the film is exposed to ethanol and then dried with nitrogen. The unpolymerized part is washed away whereas the polymerized part cannot be washed away and changes its color to red which shows fluorescence (see Figure 9c,d). This kind of microstructure may have applications in selective adsorption of other species[40] and in optoelectronic devices.[41]

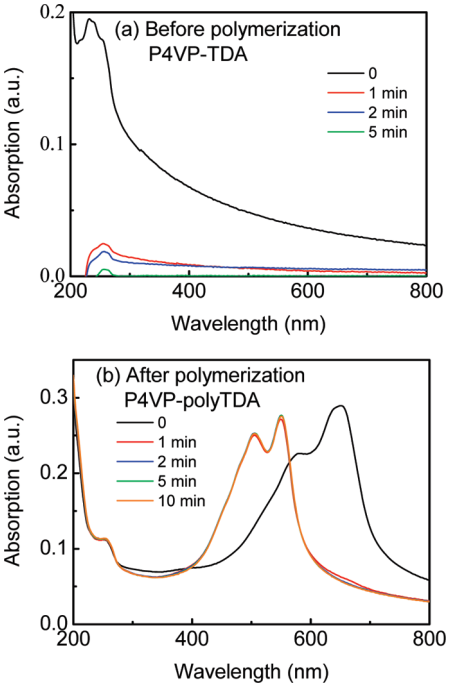

Figure 8. UV−vis absorption spectra of (a) P4VP−TDA film and (b) P4VP−polyTDA film recorded after various exposed time to ethanol.

The well-known thermochromism of PDAs is also observed in the hydrogen-bonding complex. The blue phase PDA in P4VP−polyTDA changes to the red phase of PDA after heating to 100 °C. The color does not change back to blue after cooling to room temperature. Therefore, this irreversible thermochromism in the hydrogen-bonding complex can be used to fabricate patterns with different PDA phases. The fabrication process is shown in Figure 10. In the first step, the film is irradiated with a photomask. The photopolymerization of the irradiated part takes place. In the second step, the film is heated to 100 °C. The color of the polymerized part changes to red. In the third step, the film is

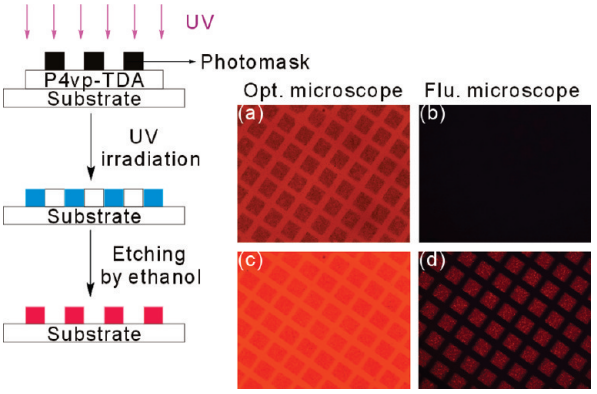

Figure 9. Process of fabrication of P4VP−polyTDA pattern by photolithography and the optical and fluorescent microscopy images of the patterns. Optical microscopy image (a) and fluorescent microscopy image (b) of the blue pattern after UV irradiation with a photomask. Optical microscopy image (c) and fluorescent microscopy image (d) of the pattern after etching by ethanol and drying by nitrogen. The photomask is 300 mesh, and the edge of every square in the images is 60 μm.

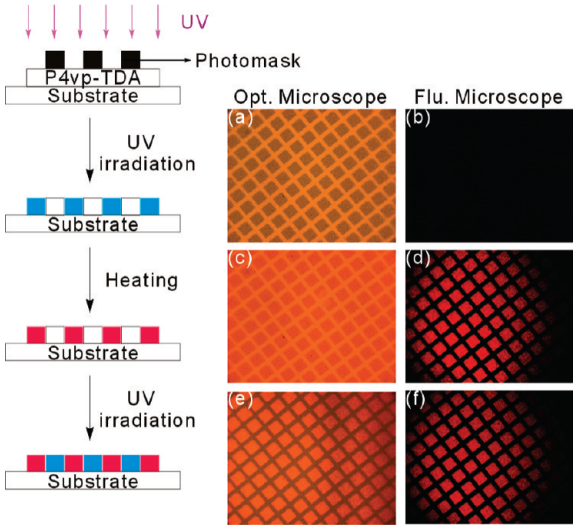

Figure 10. Process of fabrication of P4VP−polyTDA patterns with different PDA phases and the optical and fluorescent microscopy images of the patterns. Optical microscopy image (a) and fluorescent microscopy image (b) of the blue pattern after UV irradiation with a photomask. Optical microscopy image (c) and fluorescent microscopy image (d) of the pattern after heating. Optical microscopy image (e) and fluorescent microscopy image (f) of the pattern after irradiation again without photomask. The photomask is 400 mesh, and the edge of every square in the images is 45 μm.

cooled to room temperature, and the unpolymerized part is polymerized to form a blue phase PDA upon UV irradiation. As shown in Figure 10, a kind of pattern with both red phase and blue phase PDA can be fabricated after the treatment above. This process could enable to fabricate a phase grating in thin films of the hydrogen-bonding complex by using either an appropriate photomask or the interference of light.

4. Conclusion

In summary, we demonstrate stability improvements of thin films of polydiacetylenes by means of hydrogen bonding with P4VP. We show that the stable hydrogen-bonding complex can be used in photolithography and as a sensor to discriminate between various liquids and gases due to the stimuli-induced color changes of PDAs. The hydrogen-bonding complex is easy to prepare from common commercial components by processing from an environmentally friendly alcohol solution using spin-coating. The hydrogen bonds are formed by attaching different diacetylene acids to P4VP, thus allowing for tuning the kind of diacetylene derivatives easily. The solvent stability of the hydrogen-bonding complex not only provides platforms for fabrication of microstructures by photolithography but also provides the possibility of preparing a second functional layer on top of the hydrogen-bonding complex by spin-coating from organic solvents.

Acknowledgment. This work is partly supported by National Natural Science Foundation of China (No. 50703075, 50773075, and 50533040), the Chinese Academy of Sciences (kjcx3.sywH02 and kjcx2-yw-m11), and National Basic Research Program of China (No. 2006cb302900). S. Wu gratefully acknowledges financial support from the joint doctoral promotion program of the Chinese Academy of Sciences and the Max Planck Society. The authors thank Dr. J. Zhang (MPIP) for helpful discussions, M. Steiert (MPIP) for the SAXD measurements, and J. Zuo (USTC) for the measurement of the Raman spectrum.

Supporting Information Available: UV−vis absorption spectra, color pictures, FT-IR spectra, and Raman spectrum. This material is available free of charge via the Internet at http://pubs.acs.org.

References and Notes

(1) (a) Lehn, J.-M. In *Supramolecular Chemistry—Concepts and Perspectives*; VCH: Weinheim, 1995. (b) Steed, J. W.; Atwood, J. L. In *Supramolecular Chemistry*; John Wiley & Sons: New York, 2000. (c) Brunsveld, L.; Folmer, B. J. B.; Meijer, E. W.; Sijbesma, R. P. *Chem. Rev.* **2001**, *101*, 4071–4097.
(2) Lehn, J.-M. *Angew. Chem., Int. Ed. Engl.* **1990**, *29*, 1304–1319.
(3) Jeffrey, G. A. In *An Introduction to Hydrogen Bonding*; Oxford University Press: Oxford, 1997.
(4) (a) Keller, U.; Müllen, K.; DeFeyter, S.; DeSchryver, F. C. *Adv. Mater.* **1996**, *6*, 490–493. (b) Dankers, P. Y. W.; Harmsen, M. C.; Brouwer, L. A.; van Luyn, M. J. A.; Meijer, E. W. *Nat. Mater.* **2005**, *4*, 568–574. (c) Valkama, S.; Kosonen, H.; Ruokolainen, J.; Haatainen, T.; Torkkeli, M.; Serimaa, R.; Ten Brinke, G.; Ikkala, O. *Nat. Mater.* **2004**, *3*, 872–876. (d) Lauher, J. W.; Fowler, F. W.; Goroff, N. S. *Acc. Chem. Res.* **2008**, *41*, 1215–1229.
(5) (a) Wang, Y.; Wang, C.; Wang, X.; Guo, Y.; Xie, B.; Cui, Z.; Liu, L.; Xu, L.; Zhang, D.; Yang, B. *Chem. Mater.* **2005**, *17*, 1265–1268. (b) Mamiya, J.; Yoshitake, A.; Kondo, M.; Yu, Y.; Ikeda, T. *J. Mater. Chem.* **2008**, *18*, 63–65. (c) Zimmerman, S. C.; Zeng, F.; Reichert, D. E. C.; Kolotuchin, S. V. *Science* **1996**, *271*, 1095–1098. (d) Madueno, R.; Räisänen, M. T.; Silien, C.; Buck, M. *Nature (London)* **2008**, *454*, 618–621. (e) Priimagi, A.; Kaivola, M.; Rodriguez, F. J.; Kauranen, M. *Appl. Phys. Lett.* **2007**, *90*, 121103. (f) Heus, H. A.; Pardi, A. *Science* **1991**, *253*, 191–194. (g) Grubmüller, H.; Heymann, B.; Tavan, P. *Science* **1996**, *271*, 191–194. (h) Kool, E. T.; Morales, J. C.; Guckian, K. M. *Angew. Chem., Int. Ed.* **2000**, *39*, 990–1009. (i) Harigai, M.; Kataoka, M.; Imamoto, Y. *J. Am. Chem. Soc.* **2006**, *128*, 10646–10647. (j) Sun, Z.; McLaughlin, L. W. *J. Am. Chem. Soc.* **2007**, *129*, 12531–12536. (k) Joh, N. H.; Min, A.; Faham, S.; Whitelegge, J. P.; Yang, D.; Woods, V. L.Jr; Bowie, J. U. *Nature (London)* **2008**, *453*, 1266–1272. (l) Ober, C. K.; Wegner, G. *Adv. Mater.* **1997**, *9*, 17–31.
(6) (a) Okada, S.; Peng, S.; Spevak, W.; Charych, D. *Acc. Chem. Res.* **1998**, *31*, 229–239. (b) McQuade, D. T.; Pullen, A. E.; Swager, T. M. *Chem. Rev.* **2000**, *100*, 2537–2574. (c) Schott, M. *J. Phys. Chem. B* **2006**, *110*, 15864–15868. (d) Carpick, R. W.; Sasaki, D. Y.; Marcus, M. S.; Eriksson, M. A.; Burns, A. R. *J. Phys.: Condens. Matter* **2004**, *16*, R679–R697.
(7) (a) Lu, Y.; Yang, Y.; Sellinger, A.; Lu, M.; Huang, J.; Fan, H.; Haddad, R.; Lopez, G.; Burns, A. R.; Sasaki, D. Y.; Shelnutt, J.; Brinker, C. J. *Nature (London)* **2001**, *410*, 913–197. (b) Yang, Y.; Lu, Y.; Lu, M.; Huang, J.; Haddad, R.; Xomeritakis, G.; Liu, N.; Malanoski, A. P.; Sturmayr, D.; Fan, H.; Sasaki, D. Y.; Assink, R. A.; Shelnutt, J. A.;

van Swol, F.; Lopez, G. P.; Burns, A. R.; Brinker, C. J. *J. Am. Chem. Soc.* **2003**, *125*, 1269–1277.
(8) (a) Gu, Y.; Cao, W.; Zhu, L.; Chen, D.; Jiang, M. *Macromolecules* **2008**, *41*, 2299–2303. (b) Kim, J.-M.; Lee, J.-S.; Choi, H.; Sohn, D.; Ahn, D. J. *Macromolecules* **2005**, *38*, 9366–9376. (c) Lee, S.; Kim, J.-M. *Macromolecules* **2007**, *40*, 9201–9204. (d) Park, H.; Lee, J.-S.; Choi, H.; Anh, D. J.; Kim, J.-M. *Adv. Funct. Mater.* **2007**, *17*, 3447–3455. (e) Yuan, Z.; Lee, C.-W.; Lee, S.-H. *Angew. Chem., Int. Ed.* **2004**, *43*, 4197–4200. (f) Ahn, D. J.; Chae, E.-H.; Lee, G. S.; Shim, H.-Y.; Chang, T.-E.; Ahn, K.-D.; Kim, J.-M. *J. Am. Chem. Soc.* **2003**, *125*, 8976–8977. (g) Hammond, P. T.; Rubner, M. F. *Macromolecules* **1997**, *30*, 5773–5782. (h) Huang, X.; Jiang, S.; Liu, M. *J. Phys. Chem. B* **2005**, *109*, 114–119. (i) Saremi, F.; Maassen, E.; Tieke, B.; Jordan, G.; Rammensee, W. *Langmuir* **1995**, *11*, 1068–1071.
(9) (a) Peng, H.; Tang, J.; Pang, J.; Chen, D.; Yang, L.; Ashbaugh, H. S.; Brinker, C. J.; Yang, Z.; Lu, Y. *J. Am. Chem. Soc.* **2005**, *127*, 12782–12783. (b) Peng, H.; Tang, J.; Yang, L.; Pang, J.; Ashbaugh, H. S.; Brinker, C. J.; Yang, Z.; Lu, Y. *J. Am. Chem. Soc.* **2006**, *128*, 5304–5305.
(10) (a) Tamura, H.; Mino, N.; Ogawa, K. *Thin Solid Films* **1989**, *179*, 33–39. (b) Mino, N.; Tamura, H.; Ogawa, K. *Langmuir* **1992**, *8*, 594–598. (c) Cheng, Q.; Stevens, R. C. *Langmuir* **1998**, *14*, 1974–1976. (d) Cheng, Q.; Yamamoto, M.; Stevens, R. C. *Langmuir* **2000**, *16*, 5333–5342. (e) Song, J.; Cheng, Q.; Kopta, S.; Stevens, R. C. *J. Am. Chem. Soc.* **2001**, *123*, 3205–3213. (f) Kew, S. J.; Hall, E. A. H. *Anal. Chem.* **2006**, *78*, 2231–2238. (g) Jonas, U.; Shah, K.; Norvez, S.; Charych, D. H. *J. Am. Chem. Soc.* **1999**, *121*, 4580–4588.
(11) Tashiro, K.; Nishimura, H.; Kobayashi, M. *Macromolecules* **1996**, *29*, 8188–8196.
(12) (a) Kolusheva, S.; Shahal, T.; Jelinek, R. *J. Am. Chem. Soc.* **2000**, *122*, 776–780. (b) Lee, J.; Kim, H.-J.; Kim, J. *J. Am. Chem. Soc.* **2008**, *130*, 5010–5011.
(13) (a) Batchelder, D. N. *Contemp. Phys.* **1988**, *29*, 3–31. (b) Chance, R. R. *Macromolecules* **1980**, *13*, 396–398. (c) Nava, A. D.; Thaku, M.; Tonelli, A. E. *Macromolecules* **1990**, *23*, 3055–3063.
(14) (a) Charych, D. H.; Nagy, J. O.; Spevak, W.; Bednarski, M. D. *Science* **1993**, *261*, 585–588. (b) Niwa, M.; Ishida, T.; Kato, T.; Higashi, N. *J. Mater. Chem.* **1998**, *8*, 1697–1701.
(15) Ma, G.; Müller, A. M.; Bardeen, C. J.; Cheng, Q. *Adv. Mater.* **2006**, *18*, 55–60.
(16) (a) Nishide, J.; Oyamada, T.; Akiyama, S.; Sasabe, H.; Adachi, C. *Adv. Mater.* **2006**, *18*, 3120–3124. (b) Scott, J. C.; Samuel, J. D. J.; Hou, J. H.; Rettner, C. T.; Miller, R. D. *Nano Lett.* **2006**, *6*, 2916–2919. (c) Manaka, T.; Kohn, H.; Ohshima, Y.; Lim, E.; Iwamoto, M. *Appl. Phys. Lett.* **2007**, *90*, 171119. (d) Krol, D. M.; Thakur, M. *Appl. Phys. Lett.* **1990**, *56*, 1406–1408. (e) Grando, D.; Sottini, S.; Banfi, G. P.; Fortusini, D.; LoPapa, M. *Appl. Phys. Lett.* **1999**, *74*, 3601–3603. (f) Gan, H.; Liu, H.; Li, Y.; Zhao, Q.; Li, Y.; Wang, S.; Jiu, T.; Wang, N.; He, X.; Yu, D.; Zhu, D. *J. Am. Chem. Soc.* **1999**, *121*, 4580–4588.
(17) Morigaki, K.; Baumgart, T.; Jonas, U.; Offenhäusser, A.; Knoll, W. *Langmuir* **2002**, *18*, 4082–4089.
(18) (a) Yoon, J.; Chae, S. K.; Kim, J.-M. *J. Am. Chem. Soc.* **2007**, *129*, 3038–3039. (b) Yoon, J.; Jung, Y.-S.; Kim, J.-M. *Adv. Funct. Mater.* **2009**, *19*, 209–214.
(19) (a) Morigaki, K.; Baumgart, T.; Offenhäusser, A.; Knoll, W. *Angew. Chem., Int. Ed.* **2001**, *40*, 172–174. (b) Morigaki, K.; Schönherr, H.; Frank, C. W.; Knoll, W. *Langmuir* **2003**, *19*, 6994–7002.
(20) Motschmann, H.; Möhwald, H. In *Handbook of Applied Surface and Colloid Chemistry*; John Wiley & Sons: New York, 2001; Chapter 28.
(21) Gill, I.; Ballesteros, A. *Angew. Chem.* **2003**, *115*, 3386–3389.
(22) Wu, S.; Niu, L.; Shen, J.; Zhang, Q.; Bubeck, C. *Macromolecules* **2009**, *42*, 362–367.
(23) Fitrilawati, F.; Tjia, M. O.; Pfeiffer, S.; Hörhold, H.-H.; Deutesfeld, A.; Eichner, H.; Bubeck, C. *Opt. Mater.* **2002**, *21*, 511–519.
(24) (a) Wang, L.; Wang, Z.; Zhang, X.; Shen, J. *Macromol. Rapid Commun.* **1997**, *18*, 509–514. (b) Wang, M.; Zhang, G.; Chen, D.; Jiang, M.; Liu, S. *Macromolecules* **2001**, *34*, 7172–7178. (c) Duan, H.; Kuang, M.; Wang, J.; Chen, D.; Jiang, M. *J. Phys. Chem. B* **2004**, *108*, 550–555. (d) Stewart, D.; Imrie, C. T. *Macromolecules* **1997**, *30*, 877–884. (e) Odinokovo, S. E.; Mashkovsky, A. A.; Glazunov, V. P.; Iogansen, A. V.; Rassadin, B. V. *Spectrochim. Acta* **1976**, *32A*, 1355–1363. (f) Kato, T.; Kihara, H.; Uryu, T.; Fujishima, A.; Frbchets, J. M. J. *Macromolecules* **1992**, *25*, 6836–6841. (g) Kuang, M.; Duan, H.; Wang, J.; Chen, D.; Jiang, M. *Chem. Commun.* **2003**, *4*, 496–497.
(25) (a) Gao, J.; He, Y.; Liu, F.; Zhang, X.; Wang, Z.; Wang, X. *Chem. Mater.* **2007**, *19*, 3877–3881. (b) Gao, J.; He, Y.; Xu, H.; Song, B.; Zhang, X.; Wang, Z.; Wang, X. *Chem. Mater.* **2007**, *19*, 14–17.
(26) (a) Cui, L.; Zhao, Y. *Chem. Mater.* **2004**, *16*, 2076–2082. (b) Cui, L.; Dahmane, S.; Tong, X.; Zhu, L.; Zhao, Y. *Macromolecules* **2005**, *38*, 2076–2084. (c) Huang, W.; Han, C. D. *Polymer* **2006**, *47*, 4400–4410. (d) Huang, W.; Han, C. D. *Macromolecules* **2006**, *39*, 4735–4745.
(27) (a) Goswami, S.; Dey, S.; Maity, A. C.; Jana, S. *Tetrahedron Lett.* **2005**, *46*, 1315–1318. (b) Ikeda, M.; Nobori, T.; Schmutz, M.; Lehn, J. *Chem.—Eur. J.* **2005**, *11*, 662–668.
(28) Liu, X.; Jiang, M. *Angew. Chem., Int. Ed.* 2006, *45*, 3846−3850, Supporting Information.
(29) Xiao, S.; Lu, X.; Lu, Q. *Macromolecules* **2007**, *40*, 7944–7950.
(30) Lieser, G.; Tieke, B.; Wegner, G. *Thin Solid Films* **1980**, *68*, 77–90.
(31) Wegner, G. *Makromol. Chem.* **1972**, *154*, 35–48.
(32) Sixl, H. *Adv. Polym. Sci.* **1984**, *63*, 49–90.
(33) (a) Tieke, B.; Graf, H. J.; Wegner, G.; Naegele, B.; Ringsdorf, H.; Banerjie, A.; Day, D.; Lando, J. B. *Colloid Polym. Sci.* **1977**, *255*, 521–531. (b) Koch, H.; Ringsdorf, H. *Macromol. Chem. Phys.* **1981**, *182*, 255–259.
(34) Tieke, B.; Wegner, G.; Naegele, D.; Ringsdorf, H. *Angew. Chem., Int. Ed.* **1976**, *15*, 764–765.
(35) Ringsdorf, H.; Schlarb, B.; Venzmer, J. *Angew. Chem., Int. Ed.* **1988**, *27*, 113–158.
(36) (a) Jiao, H.; Goh, S. H.; Valiyaveettil, S. *Langmuir* **2002**, *18*, 1368–1373. (b) Aitipamula, S.; Nangia, A. *Chem.—Eur. J.* **2005**, *11*, 6727–6742. (c) Lin, Y.; Zhang, K.; Dong, Z.; Dong, L.; Li, Y. *Macromolecules* **2007**, *40*, 6257–6267.
(37) (a) Kuo, T.; O'Brien, D. F. *J. Am. Chem. Soc.* **1988**, *111*, 7571–7572. (b) Rhodes, D. G.; Frankel, D. A.; Kuo, T.; O'Brien, D. F. *Langmuir* **1994**, *10*, 267–275.
(38) (a) George, M.; Weiss, R. G. *Chem. Mater.* **2003**, *15*, 2879–2888. (b) Angkaew, S.; Wang, H.-Y.; Lando, J. B. *Chem. Mater.* **1994**, *6*, 1444–1451.
(39) (a) Sellinger, A.; Weiss, P. M.; Nguyen, A.; Lu, Y.; Assink, R. A.; Gong, W.; Brinker, C. J. *Nature (London)* **1998**, *394*, 256–260. (b) Nguyen, T. Q.; Wu, J.; Doan, V.; Schwartz, B. J.; Tolbert, S. H. *Science* **2000**, *288*, 652–656. (c) Podsiadlo, P.; Kaushik, A. K.; Arruda, E. M.; Waas, A. M.; Shim, B. S.; Xu, J.; Nandivada, H.; Pumplin, B. G.; Lahann, J.; Ramamoorthy, A.; Kotov1, N. A. *Science* **2007**, *318*, 80–83. (d) Capadona, J. R.; Shanmuganathan, K.; Tyler, D. J.; Rowan, S. J.; Weder, C. *Science* **2008**, *319*, 1370–1374.
(40) Shi, F.; Dong, B.; Qiu, D.; Sun, J.; Wu, T.; Zhang, X. *Adv. Mater.* **2002**, *14*, 805–809.
(41) (a) del Campo, A.; Arzt, E. *Chem. Rev.* **2008**, *108*, 911–945. (b) Sun, Y.; Forrest, S. R. *Nat. Photonics* **2008**, *2*, 483–487. (c) Gather, M. C.; Köhnen, A.; Falcou, A.; Becker, H.; Meerholz, K. *Adv. Funct. Mater.* **2007**, *17*, 191–200.